Growth of stabilized γ-Fe films and their magnetic properties

A. Kirilyuk,* J. Giergiel, J. Shen, M. Straub, and J. Kirschner
Max-Planck Institut für Mikrostrukturphysik, Weinberg 2, D-06120 Halle(Saale), Germany
(Received 5 October 1996)

Ultrathin γ-Fe/Cu(001) films are unstable with respect to the fcc→bcc phase transition with the reported onset of transformation as early as at 5 ML. Here we demonstrate that with the help of a collaborative surfactant effect of carbon and oxygen, γ-Fe films up to more than 60 ML thickness can easily be produced. The interstitial incorporation of carbon atoms into the fcc lattice is the main reason for this stabilizing effect. Oxygen plays a very important role in improving the layer-by-layer growth. This strong surfactant effect of oxygen, however, reveals itself only in the presence of carbon. The interstitial carbon does not influence the magnetic properties of fcc iron significantly, except for the surface anisotropy value. [S0163-1829(96)05526-9]

INTRODUCTION

Ultrathin iron films on top of a single crystal Cu(001) substrate have become a system intensively studied for several years. Initial interest in that subject is due to the fact that the γ-Fe phase, having fcc crystallographic structure, only occurs at high temperatures (between 1184 K and 1665 K). This fcc iron does not reveal any ordered magnetic structure in this high temperature range. However, extrapolating to lower temperatures the theory predicts two magnetic phases possible depending on the atomic volume:[1] ferromagnetic (FM) with a lattice constant of 3.64 Å (atomic volume 12.1 Å^3), and antiferromagnetic (AFM) with 3.57 Å (11.7 Å^3).

One of the possibilities of stabilizing a novel phase is to grow a thin epitaxial film on an appropriate substrate. For the γ-Fe phase, a copper single crystal (fcc, $a=3.61$ Å) should fit ideally because of the small epitaxial misfit ($\approx$ 1%) for both FM and AFM iron phases. Which phase the system then prefers depends on many parameters, mostly unknown. The Cu(001)-oriented surface is especially suitable for such studies because it can be prepared smooth, with large ($>$ 500 nm) atomically flat terraces.[2]

However, even an almost ideal substrate like that implies several problems. On the one hand, the heterogeneity of the system leads to alloying, intermixing, layering, etc. Usually the growth mode and surface morphology of the given system are to a large extent determined by these factors. Fortunately, alloying most probably could be neglected: the bulk miscibility of Cu in both γ-and α-Fe is small, i.e., less than a few percent at $\approx$1200 K, and correspondingly smaller at lower temperatures.[3] Similar solubility values are reported for Fe in Cu. Thus, from this point of view we might expect sharp Cu/Fe interfaces. It should be mentioned, however, that surface material properties may be different from bulk ones, and some interface alloying and/or intermixing might be detected even in this case.[4,5]

Important parameters determining the growth mode are surface (σ_{Fe}, σ_{Cu}) and interface ($\sigma_{\mathrm{Fe\text{-}Cu}}$) free energies. Reliable data are difficult to obtain. However, the best estimation indicates[6] that

$$\sigma_{\mathrm{Fe}} > \sigma_{\mathrm{Cu}} + \sigma_{\mathrm{Fe\text{-}Cu}} \qquad (1)$$

and hence the system may prefer the agglomeration growth mode. Nevertheless, the thermodynamic equilibrium implicit in such a simple consideration is very difficult to realize experimentally, and the growth is often determined by kinetic limitations. Indeed, as has recently been shown,[5] the Fe/Cu system prefers to be in a sandwich configuration Cu/Fe/Cu according to Eq. (1), if a special annealing treatment is applied. Under the condition of room temperature (RT) growth, the system does not approach this state.

The epitaxial misfit problem also arises as a result of a heterogeneous system. As was pointed out above, our case is quite favorable as the epitaxial misfit value is quite small ($\sim$1% in any case). Such values are not expected to cause dislocation formation below a film thickness of some 20 ML.[7] Fe/Cu can be compared with a similar system, viz., Co/Cu, where quasi-layer-by-layer growth is observed at least up to 20 ML, in spite of 3.9% epitaxial misfit.[8] Thus misfit should not influence the growth very much.

On the other hand, it is very important that the γ-Fe phase is thermodynamically unstable at room temperature [the difference with α-Fe is some 0.02 eV/atom (Ref. 9)]. Therefore the phase cannot exist without the stabilizing action of the Cu substrate, and, naturally, at a certain film thickness it will transform to the bcc structure. This incipient transformation appears to primarily determine the structure and morphology of the grown films.[10] Other factors (considered above) also play their certain roles, particularly if different growth temperatures are considered.

In room temperature growth three different growth regions have been identified.[11]

(1) 0–4 ML thickness: small islands; the structure appears to be tetragonally distorted, showing a complicated type of reconstruction.[12,13]

(2) 5–10 ML thickness: large islands, reasonably good layer-by-layer growth. The structure is relaxed to a smaller lattice parameter (3.57 Å).[12–14] These are not simple misfit dislocations but thin elongated bcc phase inclusions,[10] which are responsible for the observed relaxation. Temperature cycling down and back to RT also seems to produce some dislocation networks.[15] However, in this region the bcc phase occupies only a small part ($\lesssim$1–2%, slightly more for 10 ML) of the total sample area.

(3) >11 ML thickness: in the region of 10–11 ML the fcc-to-bcc phase transformation proceeds rapidly, and above 12 ML in thickness the films predominantly are of bcc structure. Their surface is very rough as it is difficult for the bcc Fe phase to adopt the structure of the fcc Cu template.

Now let us recall the magnetic properties of this epitaxially stabilized γ-Fe phase. They received much attention in recent years[11,16–23] and demonstrate an extreme sensitivity of the magnetism to the film structure and morphology. It appeared that the preparation procedure is also important, so we consider below only RT growth, where the magnetic properties happen to be very closely related to the growth modes described above.

Films belonging to the first region clearly show the FM type of ordering with the magnetization in perpendicular orientation to the film plane. The Kerr ellipticity value increases linearly with the film thickness in this region,[11] indicating the homogeneous magnetization of all iron atomic planes. This FM order is explained by large atomic volumes: at these thicknesses the lattice is expanded both in plane and in between the planes,[13] approaching the values theoretically calculated.[1]

In the second region the magnetization suddenly drops, remaining constant for all film thicknesses of that region. The value of the Kerr ellipticity corresponds to the presence of two FM layers, probably lying at the top of the film. This fact is explained by surface layer relaxation leading to the increase of the first interlayer spacing. Apart from the top two layers, the rest of the film is nonmagnetic at temperatures above 200 K. Recently, it has been supposed that the AFM type of ordering (more precisely, an AFM spin wave of a 2.6 ML period) appears below 200 K for these lower-lying layers,[16] which is in full agreement with theoretical predictions[1] for such a low-atomic-volume phase. Nevertheless, the described model cannot be considered as experimentally fully established because it is difficult to prove such a wave across a region of some 5 ML (between 5 and 10 ML). One should also note that in small γ-Fe particles precipitating inside the Cu single crystal matrix, this AFM ordering is usually observed at much lower temperatures, i.e., at about 60 K.[24,25]

Magnetism changes again in the third region: the magnetization flips to the film plane (crystallographic direction of the Cu substrate [110]), and again the whole film becomes homogeneously magnetized. These are the original properties of the α-Fe phase, which is the only one existing at these thicknesses.

This strong dependence of the magnetic properties on film structure plus the complexity introduced by the intrinsic film structure instability makes it difficult to study the magnetism of γ-Fe. Therefore a better stabilization of the γ-Fe phase (and larger film thicknesses) would be very desirable. One possibility is to use a better substrate. Some experiments have been performed with thin iron films grown on the $Cu_3Au(100)$ substrate[26,27] (fcc, $d=3.75$ Å). Although it seems to stabilize the FM phase of iron, the growth mode is far from ideal. In general, the substrate choice is limited to very few materials having appropriate structure parameters and thermodynamic properties.

The next thing to do is to add something *inside* the grown film, with this additive possibly stabilizing the fcc phase. Since we are interested in magnetism, attention should be paid to the influence of those additives on the magnetic properties of the material. On the other hand, this Fe-X (X is the additive atom) solution should have a fcc structure and reveal more thermodynamic stability than the original γ-Fe phase does. If we consider the Fe-C binary phase diagram,[28] we notice that γ-Fe with 3.12 at. % of carbon is stable already at 1009 K instead of 1184 K. Another important fact is that this dissolved carbon incorporates interstitially, increasing the lattice constant isotropically.[3] Thus, starting from 3.57 Å for pure Fe, about 6 at. % of incorporated carbon produces an ideal fit to the Cu substrate. This would eliminate (or minimize) another kind of instability related to the lattice misfit. From the magnetic point of view, there are some indications[29] that interstitial carbon does not influence the magnetic moment of iron. However, such a macroscopic quantity as, e.g., the coercive field H_c is strongly influenced by even a slight carbon contamination for the bcc phase.[30] This is not important if fundamental magnetic properties are considered. We will discuss this question below when studying the magnetism of our samples.

The proposed stabilizing procedure is as follows. We add some carbon to the growing iron film. We do not know yet how much we need, probably some 3–6 at. %. The carbon solubility in γ-Fe is quite high (up to 8.9 at. %), which is due to the large size of octahedral interstices (0.52 Å) where the carbon atoms can be introduced. In contrast, the carbon solubility in α-Fe is small, only 0.095 at. %, because of the interstices being smaller (tetrahedral ones, 0.36 Å). Any subsequent $\gamma \rightarrow \alpha$ transition would require carbon precipitation from the whole film, an unlikely process at room temperature. This is basically the reason for the extended stability of the fcc C-Fe phase. At the same time, the interstitial carbon expands the fcc iron lattice, thus resulting in a better fit to the Cu substrate. Therefore the fcc C-Fe films will be stabilized for a larger thickness range.

To add some carbon to the growing film, different carbon-containing gases can be used, which are known to easily dissociate on metal surfaces. Thus we have chosen ethylene, C_2H_4, and acetylene, C_2H_2. There is a large list of literature published about adsorptive and dissociative properties of these gases.[31–33] We use also methane, CH_4, for the sake of comparison with other transition metal surfaces, with its sticking coefficient being reported[34] to be of the order of 10^{-8}, which is just zero for our purposes. Next, carbon monoxide has been proved to produce some stabilizing effect,[35,36] although another study has shown that only reversible molecular adsorption of CO could be detected on the γ-Fe surface.[37] To elucidate this ambiguity we have also performed studies using CO.

In principle, it is also possible to improve the growth mode of the film (but only the growth mode, not stability) with the help of a surfactant. The usual effect is interlayer transport enhancement by either reducing the step-crossing barriers or by increasing the nucleation density.[38] At the initial stage of Fe growth some similar effect has been detected with oxygen acting as a surfactant.[39,4] That is why in our studies we also included oxygen, both alone and in mixtures with other gases.

Therefore, in this paper we report on the structural stabilization of pseudomorphic fcc-Fe films. Films of high surface

quality and more than 60 ML thick were grown on a Cu(001) substrate. Such a stabilization was attained by adding small amounts of interstitial carbon. Additional oxygen revealed an unusually strong surfactant effect, involving both carbon and oxygen at the same time. To the best of our knowledge this is the first observation of a ''collaborative'' surfactant effect. The results of our study have been recently published in brief.[40]

The magnetic properties of these stabilized films, on the one hand, prove the fcc phase stabilization. On the other hand, there arose also a new effect: carbon incorporation affects the uniaxial anisotropy of the film. Detailed investigations of such films could help elucidate the magnetism of the γ-Fe phase, and, at the same time, the role of interstitials in magnetism in general.

I. EXPERIMENTAL SETUP

The experiments were performed in an ultrahigh vacuum system, equipped with an Auger Cylindrical-mirror analyzer (CMA) system, low-energy electron diffraction (LEED), medium-energy electron diffraction (MEED), and magneto-optical Kerr effect (MOKE) experimental facilities. Scanning tunneling microscope (STM) images were measured in a similar chamber. A fully automatic video-LEED system[41] has been used for recording LEED images as well as for measuring the LEED spot intensity versus electron beam energy dependencies (I/V LEED curves). For LEED studies, the earth magnetic field was compensated to better than 95% of its value with the help of a Helmholtz coil system. MEED spot intensity oscillations (specular spot under in-phase reflection conditions) were measured using the electron gun of the Auger system and the same video-LEED setup owing to the face-to-face arangement of the Auger and LEED instrumentation. Such a configuration allowed us to measure Auger spectra *in situ* without disturbing the film growth procedure, and hence from the same point of the sample where MEED intensity oscillation curves were being measured.

The sample was mounted on a three-axis manipulator, allowing the sample to be cooled down to 180 K and heated up to 1000 K. The temperature was monitored with a Chromel-Alumel (type K) thermocouple, pressed to the sample by sample holding clamps.

The sample used as a substrate for the Fe films was a polished Cu(001) single crystal disk, 1 cm in diameter and 3 mm thick, with its orientation aligned to within 0.1°. The substrate surface was prepared by Ar-ion sputtering (1 kV, $\approx 5\ \mu$ A/cm^2) and annealing in 900 K (10 min) cycles, until the surface contamination was below the CMA detection limits, and LEED exhibited a sharp (1×1) pattern with a very low background. The MEED pattern showed sharp, rounded spots, verifying that the surface consisted predominantly of atomically flat terraces (of lateral size of up to 400 nm, as measured by STM). After preparation the sample was allowed to cool at least 3 h; during film growth its temperature was 300 ± 5 K.

The deposition source consisted of 99.99% pure Fe wire heated by electron bombardment from a tungsten filament. Typically, the pressure rise in the chamber was less than 4×10^{-10} mbar when the oven was operating. A long cleaning procedure (up to 20 h) was required to outgas adsorbed gases (mostly nitrogen) from the Fe wire . Typically, the evaporation rates were 0.8–1.2 ML/min; they were monitored (and calibrated) using MEED intensity oscillations. Usually, the C and O contamination of clean films did not exceed 1–2 at. %.

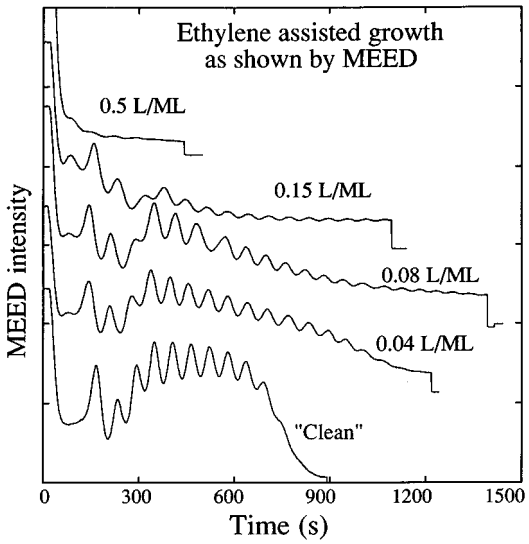

FIG. 1. MEED oscillation curves for the iron growth at different exposures of ethylene, C_2H_4 (indicated in the figure). The ethylene pressures were kept constant over the whole film growth. Optimizing the exposure (around 0.08 L/ML) leads to at least doubling the critical thickness of the fcc iron film.

To incorporate carbon into the growing film we applied partial pressures of different gases. First, we used ethylene, C_2H_4, and acetylene, C_2H_2, and also methane, CH_4, for comparison. Next, we used CO because of its known effect[35] limited growth extension by 2–3 ML has been observed previously,[11] and oxygen to possibly improve the growth mode. Mixtures of different gases were also used. The maximum partial pressure applied was determined by the ion pump saturation: if its effectivity drops down, the presence of some other gases might become important and affect the growth. Therefore partial pressures above $(3–5)\times10^{-8}$ mbar have not been applied in order to keep the pressures of other C and O-containing gases below $(1–2)\times10^{-10}$ mbar. The exposure applied to the film will be expressed in langmuirs per 1 ML of the film thickness. So the pressure of 2.2×10^{-8} mbar and the growth rate of 1 ML/min correspond to 1 L/ML.

To precisely control the gas pressure during growth, a quadrupole mass spectrometer was initially calibrated for different gases using the ion gauge vacuum meter. Therefore it was possible to monitor the partial pressure of the gas used while the evaporation oven and MEED beam were working. Otherwise this would result in the increase of the background pressure in the chamber at the cost of different other gases, hiding the pressure of interest.

II. RESULTS

We start by considering a clean-grown iron film. The well-known behavior of the MEED oscillation curve for such a growth procedure (reproduced by us) is shown in Fig. 1.

The irregularity of the oscillations for thicknesses between 0 and 4 ML is not yet understood; bilayer growth which can be supposed according to that shape (which has also been deduced from Auger measurements[42]) has been observed in real space for the low-temperature regime and only slightly for the RT growth.[19] However, for RT growth intermixing at the substrate-film interface has been derived from STM images,[4] while another STM paper shows regular layer-by-layer growth over the whole 0–10 ML thickness range.[19] Careful Auger studies reveal a nontrivial behavior of the Auger peak intensities, which may be due to both intermixing and bilayer growth. Quantitative I/V LEED studies show a very complex crystallographic structure of this region, with all layers reconstructed both in plane and vertically.[13]

In the region of 5–11 ML regular MEED oscillations indicate a good layer-by-layer growth, which is confirmed by STM images[10] showing the increase of the island size in that region. However, even here there are indications of the approaching fcc-to-bcc-phase transition. Indeed, as early as at 5 ML some bcc phase precipitates appear as thin elongated ridges. Up to 10 ML, the part of the bcc phase remains small; the only effect produced is the relaxing of the fcc structure[14] (see also the I/V LEED data in Fig. 10 below).

Above 10 ML, the transformation proceeds rapidly so that at 12 ML the film already consists of mainly the bcc phase. This is indicated by a sudden drop of the MEED intensity at this point owing to the high roughness of that bcc surface.[10]

A. Carbon incorporation

If the film is grown with some partial pressure of ethylene, C_2H_4, in the chamber, the curve of MEED oscillations changes its shape depending on the gas exposure value (see Fig. 1). Optimizing the exposure to be applied enables a quasi-layer-by-layer growth for twice as long (as deduced from the presence of MEED oscillations), i.e., up to 20–25 ML. The same effect is also produced by acetylene, C_2H_2. Thus, in some respects such a ''dirty'' growth procedure works much better than a clean one (see also Ref. 36), i.e., much thicker fcc iron films can be stabilized. However, the surface quality is decreasing with film thickness, as indicated by the decreasing MEED intensity. The STM images confirm this increase of the surface roughness: while Fig. 2 (top) is very similar to that of a clean-grown film for the same thickness (except some patches discussed below), Fig. 2 (bottom) shows the multilayer growth mode for thicker films. Thus, while for a 7.7 ML thick film there are five atomic layers simultaneously, this is not observed for clean films (cf. the STM images in Ref. 10). In contrast to clean growth, bcc phase precipitates do not appear in these images (the measured step heights correspond to the fcc phase). It is not known at which point the film transforms to bcc, as the increasing surface roughness prevents us from detecting this transition.

The dependence of Auger spectra on the film thickness (Fig. 3) shows the increase of the carbon C_{272} Auger signal (normalized by Fe_{703} and Cu_{920} peak intensities) followed by electron-escape-depth-induced saturation which is consistent with a constant rate of carbon incorporation. The carbon concentration is approximately 70% of the maximum possible value for a given pressure (i.e., if complete incorporation of every atom landing on the surface is assumed). In reality, this is almost within the possible experimental error. The carbon concentration of the film has also been found to be proportional to the applied ethylene (or acetylene) pressure, at least up to exposures of 0.2 L per monolayer.

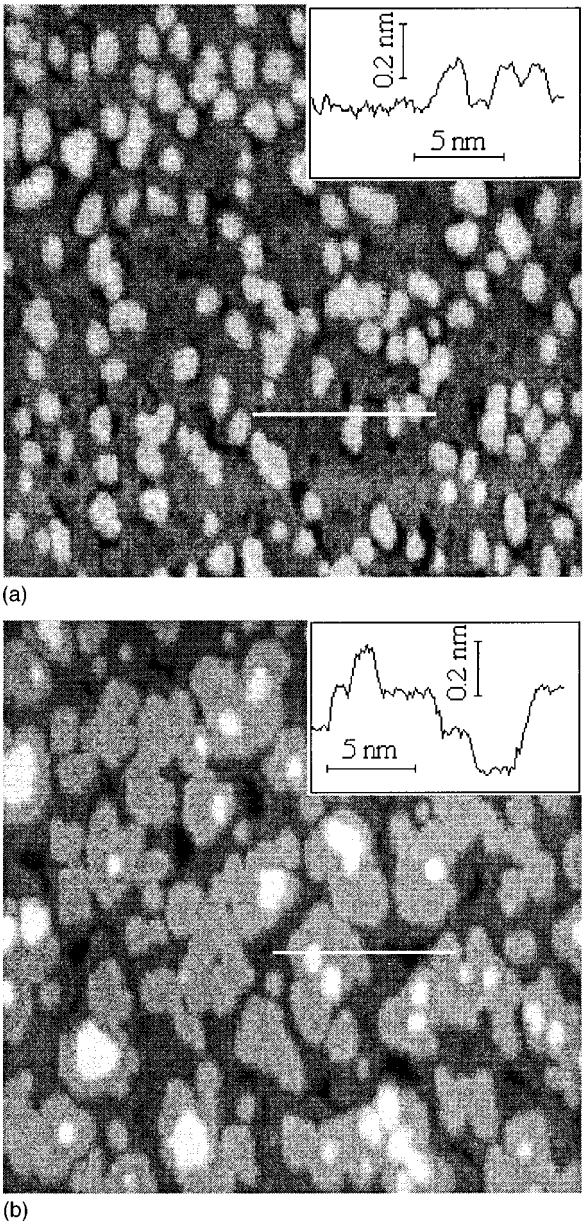

FIG. 2. STM images for films grown with acetylene: (top panel) 3.2 ML thick film; (bottom panel) 7.7 ML thick film. Unlike for nonassisted growth, here there are no elongated ridges, but a much rougher surface for thicker films (bottom panel). The step height corresponds to the fcc iron lattice. Unclear patches in the top panel are probably the hydrocarbon precipitates.

The iron-carbon binary phase diagram[28] provides the maximum equilibrium solubility of carbon in the γ-Fe phase of 8.9 at. %, i.e., this is the maximum possible concentration of the interstitial carbon. It seems that the carbon concentration in our films is higher than that (we can easily attain 20–25 at. %) so that the question of the location of the additional C arises. STM images indicate one of the possibili-

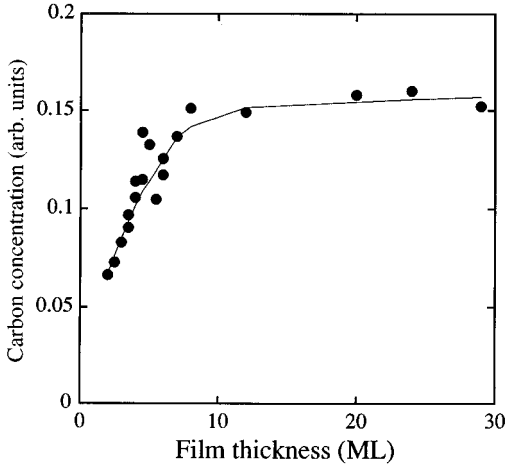

FIG. 3. Intensity of the $C_{272\,eV}$ Auger peak (normalized by $Fe_{703\,eV}$ and $Cu_{920\,eV}$ peak amplitudes) as a function of film thickness for growth under the acetylene exposure of 0.1 L/ML.

ties: at thicknesses around 3 ML some precipitates occur [those patches in Fig. 2 (top)], which might be carbon (or hydrocarbon) clusters.

LEED shows the same diffraction pattern for all measurable film thicknesses, up to 24 ML; see Fig. 4. The (2×2) superstructure visible in the pattern probably appears owing to the carbon contamination on the surface (see Auger data below). In Ref. 43, such a pattern on a Ni(001) surface is found to be caused by surface reconstruction under the influence of adsorbed carbon. One should note that owing to the strong surface roughness, the LEED pattern degrades very much with increasing film thickness. Thus no structural change has been observed in thicker films.

To check the film surface structure in more detail, we have measured the I/V LEED dependencies of acetylene-stabilized films of different thicknesses (Fig. 5). The main

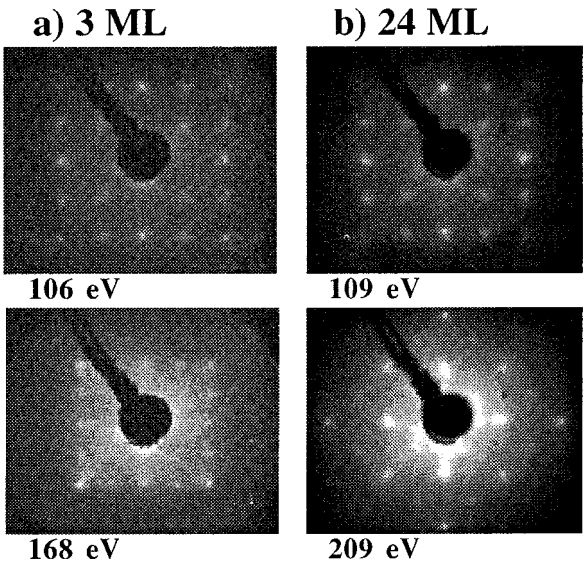

FIG. 4. LEED patterns for different thicknesses of iron films grown under the acetylene exposure of 0.08 L/ML. Note *the same* pattern for the whole thickness range from (a) 3 ML to (b) 24 ML. The (2×2) superstructure appears owing to the carbon-induced surface reconstruction.

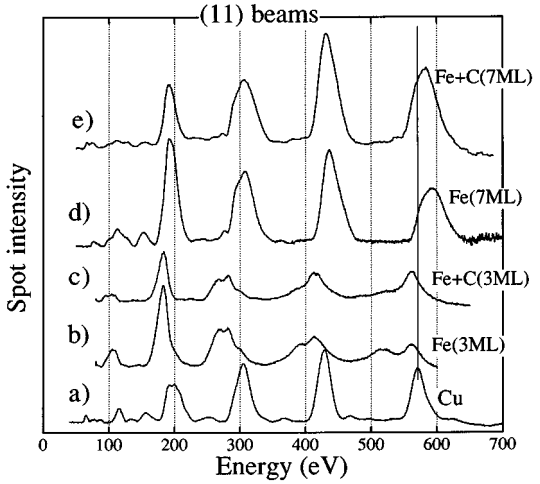

FIG. 5. I/V LEED curves [reflex (11)] for differently prepared samples: (a) clean Cu substrate; (b) clean 3 ML iron film; (c) 3 ML iron film grown under the acetylene exposure of 0.1 L/ML; (d) clean 7 ML iron film; (e) 7 ML iron film grown under acetylene exposure of 0.1 L/ML. The slight shift of the peaks on the curve (e) with respect to those of (d) shows the increase of the interlayer spacing (0.01–0.02 Å) due to the carbon incorporation.

peaks in these curves appear to be slightly shifted in the case of the films grown with C_2H_2 (thicker than 5 ML); see curve (e). In the kinematic LEED approximation, this shift signifies the increase of the interlayer spacing, i.e., the lattice seems to be expanded (it is possible to estimate the expansion as 0.01–0.02 Å) owing to the carbon. Such expansion indicates that carbon incorporates interstitially, as interstitial carbon is known to increase the γ-Fe lattice constant.[3] However, the expansion observed is not large. As mentioned above, approximately 6 at. % of incorporated carbon corresponds to the perfect match of fcc iron to copper. Our I/V curves allow the conclusion to be drawn that here only a fraction (30–50%) of this effect occurs, because the peaks in the I/V curves are shifted by only part of the distance towards the positions of Cu peaks. This is in contradiction to the fact that we have twice the necessary amount of carbon (around 12–15 at. %). Therefore we have to suppose that only a small amount of carbon incorporates interstitially, with the residual carbon possibly introduced substitutionally or forming some kind of precipitate. The reason for that might be due to the fact that ethylene and acetylene are not completely dehydrogenated at room temperature;[33] species like C_2H and CCH_3 are usually found at the surface. Of course, such molecules are difficult to introduce into small interstices. Some precipitates which in thinner films are detected by STM [Fig. 2 (top)] might be formed from such species.

If the applied gas exposure is high enough (more than 0.1 L/ML), the growth mode slightly changes at very low film thicknesses. From Fig. 1 we can conclude that the first peak in the curves of the MEED oscillations increases its amplitude. This effect should be very similar to that recently observed for oxygen.[4,39] However, no real surfactant effect is expected for these hydrocarbons as they obviously do not float at the surface when the film is growing. The situation is not very clear because STM does not always show the real

bilayer growth mode (compare Refs. 10 and 44). The same subtle effect was also observed for CO (see below).

Films grown with a partial pressure of methane, CH_4, show MEED intensity behavior indistinguishable from the ''pure'' ones (at least up to the dose of 2 L/ML). STM images (not shown here) demonstrate that the growth mode does not differ from the nonassisted growth, and the film is also undergoing the fcc→bcc phase transformation starting at 5 ML. Auger analysis revealed only a slight increase (if any) of the carbon contamination. Obviously, methane does not react with iron, not even at steps. This effect is in good agreement with the reported adsorption properties of methane:[34] its sticking coefficient is very low, of the order of 10^{-8}, or less.

Thus our hypothesis of the stabilizing effect of carbon seems to explain a good number of the observations. However, the carbon incorporated interstitially seems to be only a small part of the carbon contained in the film. Nevertheless, this is already enough to extend the critical thickness of fcc iron films at least twice compared to clean-grown samples. The rough surfaces of such stabilized films are probably due to the incomplete dissociation of ethylene or acetylene leading to some kind of cluster formation.

B. CO-assisted growth

The interaction of carbon monoxide, CO, with fcc iron surfaces appears to be a puzzling subject. On the one hand, solely reversible molecular adsorption has been detected on (001) γ-Fe surfaces up to pressures of 0.1 Pa and at temperatures up to 620 K.[37] This alone is puzzling because CO dissociates on bcc iron[45] and probably even on other fcc iron surfaces.[46,47] On the other hand, partial pressures of the order of only 7×10^{-8} Pa do already have some effect on the Fe/Cu(001) film growth.[11] Thus, to elucidate this we have extensively studied the γ-Fe/Cu(001) film growth for different CO partial pressures.

First we present the MEED data (Fig. 6). The effect is striking, especially for higher CO exposures [see curve (d)]. Now there are oscillations up to 35 ML—a threefold increase in the critical thickness relative to that regularly obtained for 11–12 ML. Moreover, at some exposures the surface quality significantly improves in the region of 10–30 ML, as indicated by the MEED intensity almost recovering its initial value. With increasing CO exposure, the character of the MEED oscillations smoothly varies from ''clean'' [curve (a)] to ''stabilized'' [curve (d)]—see the intermediate curve (b). This indicates that there is no phase change, with these films being still of the fcc phase. STM reveals a quasi-layer-by-layer growth mode up to at least 30 ML [see Fig. 7 (top)] with step heights corresponding to that of γ-Fe. The final collapse of the MEED intensity in the region of 30–35 ML is due to the fcc-to-bcc phase transformation: this is concluded from the LEED pattern showing the usual ''(3×1)'' superstructure. The STM images demonstrate a sudden surface roughening at this thickness [Fig. 7 (bottom)].

Another surprising fact here is the independence of the critical thickness of the applied CO exposure. Figure 6 shows [compare curves (c) and (d)] that doubling the exposure changes the MEED oscillations strongly but it does not result in a thicker γ-phase. This applies to the whole region of 0.1–1 L/ML. The explanation of this effect will be provided below, in Sec. II D.

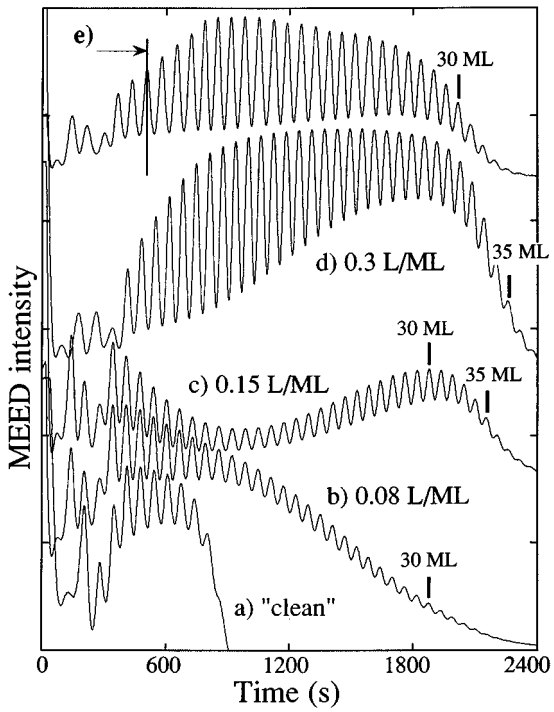

FIG. 6. MEED oscillation curves for iron growth under different exposures of CO, indicated in the figure by curves (a)-(d); dependence (e) was obtained by interrupting the CO supply [the same exposure as in (d)] at 7 ML.

To figure out the role of CO and/or of its components in changing the growth mode, surface concentrations of carbon and oxygen are of interest. Measured by Auger spectroscopy, these values are shown in Fig. 8. Plotted are the normalized Auger signals as a function of film thickness. The data strongly depend on the CO pressure. The behavior of the curves of Fig. 8 can be summarized as follows. At constant partial pressures of CO both carbon and oxygen begin to accumulate at the surface (at least, within the respective Auger probing depth — a few ML). Then, starting at some point, the carbon concentration begins to decrease, while oxygen continues increasing although more slowly. The higher the CO partial pressure applied, the shorter is this first accumulation stage, and the lower is the surface carbon concentration attainable in thick ($\approx$30 ML) films. At exposures above 0.3 L/ML the final surface carbon contamination does not exceed that of clean-grown films. At the same time, the oxygen concentration might be as high as 30–40 % of 1 ML.

Such strong difference between carbon and oxygen Auger signals can only be possible if CO is dissociated. This result clearly differs from that of Ref. 37. We checked, however, that if the film is not growing, only molecular absorption of CO is observed, in agreement with Ref. 37. This unexpectedly strong interaction of CO with Fe is suggested to be due to the dynamical conditions operative on the surface during growth. The dissociation of CO happens because of the incoming iron atoms. What they possibly do is to fix the CO molecules so that desorption becomes inhibited. As the CO molecule sticks by the carbon end, it is the C atom which is

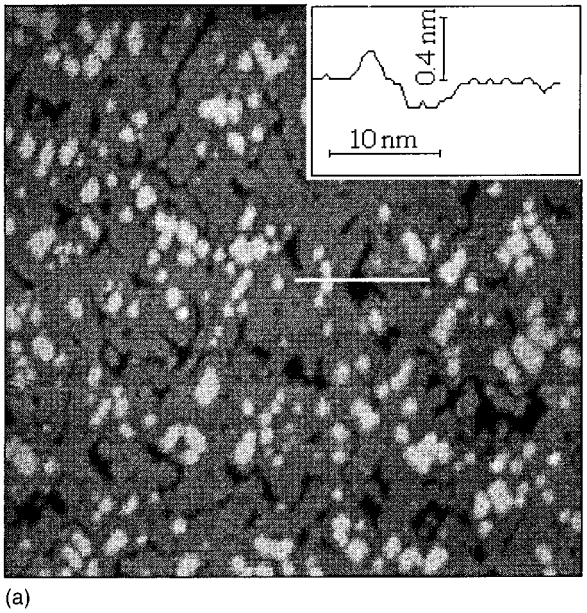

FIG. 7. STM images of the CO-assisted grown film: (top panel) 30 ML thick film—fcc phase; (bottom panel) 35 ML thick film—bcc phase. The images are 100×100 nm^2 large. Note the very high surface roughness of the latter image, especially compared to the first one.

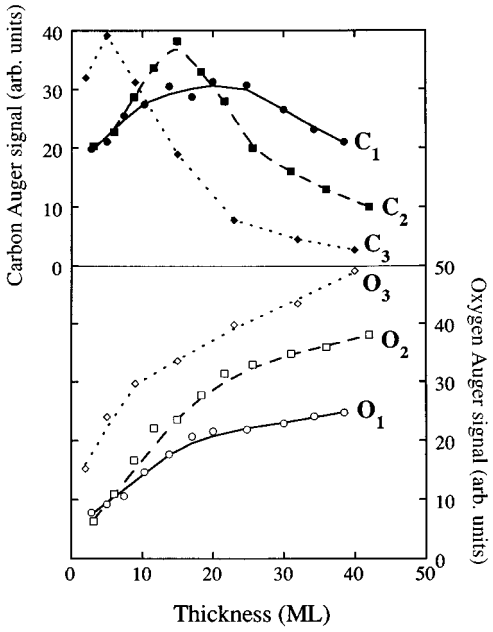

FIG. 8. Carbon and oxygen surface concentrations as a function of film thickness for the Fe film grown at (C_1, O_1) 0.08 L/ML of CO, (C_2, O_2) 0.15 L/ML of CO, and (C_3, O_3) 0.4 L/ML of CO. Plotted are the normalized carbon and oxygen Auger peak amplitudes: $C_{272}/(Fe_{703}+Cu_{920})$ for carbon (solid dots), and $O_{503}/(Fe_{703}+Cu_{920})$ for oxygen (open dots).

fixed first. Next, the C-O bond is broken, with the oxygen atom easily floating onto the surface. The dynamically increased step density is a very important factor which, together with the mechanism described above, may be responsible for dissociative chemistry that is otherwise not observed on this surface. Of course, the proposed mechanism still has to be verified experimentally.

In any case we may conclude that oxygen is floating out to the surface while carbon stays behind. The increase of the oxygen Auger peak with film thickness confirms the picture of accumulated surface oxygen. Such floating oxygen has already been observed on the γ-Fe surface.[39] The LEED results essentially confirm this picture showing the $c(2\times2)$ superstructure on top of the regular γ-Fe pattern [Fig. 9 (top)]. This $c(2\times2)$ superstructure appears only when some amount of CO is adsorbed and dissociated. It is identical to the structure induced by 1–8 L of O_2 adsorbed on the clean Fe surface [Fig. 9 (top)]. Furthermore, the energy dependence of these structures [I/V LEED data, see Fig. 9 (bottom)] is identical in both cases. This is an unlikely coincidence unless oxygen actually floats out to the surface. Thus, if the film is grown with CO, an ordered layer of oxygen is floating on the film surface.

The observed decrease of surface carbon is the direct consequence of this oxygen layer. We suppose that oxygen blocks the surface against further CO adsorption and hence against carbon uptake. A similar blocking effect has in fact been observed in the interaction of CO and O_2 on bcc Fe surfaces.[48] The oxygen and carbon concentration behavior will be discussed in more detail below (see the Appendix).

A logical conclusion can be drawn from this blocking effect. As the carbon uptake is blocked after a short growth period, it is actually not necessary to permanently supply CO. The CO supply may most probably be interrupted after some initial period, without affecting the subsequent growth. The experiment entirely confirms this suggestion. If growing the film is started under the conditions of curve (d) of Fig. 6 (i.e., at CO exposure of 0.3 L/ML), followed by an interruption of the CO supply at 7 ML (we checked that the CO pressure drops by more than one order of magnitude in a few seconds after the valve is closed), there are still oscillations up to at least 30 ML [see curve (e) of Fig. 6].

To figure out the influence of our additives on the film structure, a set of I/V LEED curves is presented for CO-stabilized films of different thicknesses, as well as for clean-grown films, and for a Cu substrate, for comparison. The results are shown in Fig. 10. As mentioned above, the posi-

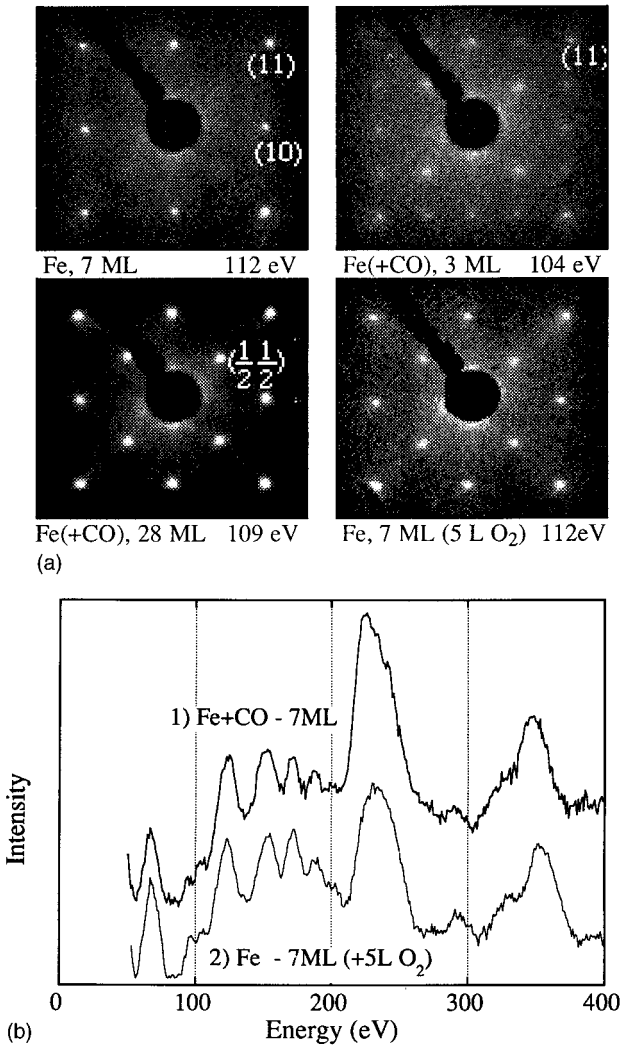

FIG. 9. (Top panel) LEED patterns for differently grown films (the way of preparation is indicated in the figure; the exposure used for the CO-assisted growth was 0.3 L/ML) at nearly the same electron energy of around 110 eV, and (bottom panel) I/V LEED dependencies for $c(2\times2)$ superstructure spots on different samples: (1) grown with CO, and (2) clean grown, then saturated with 5 L O_2.

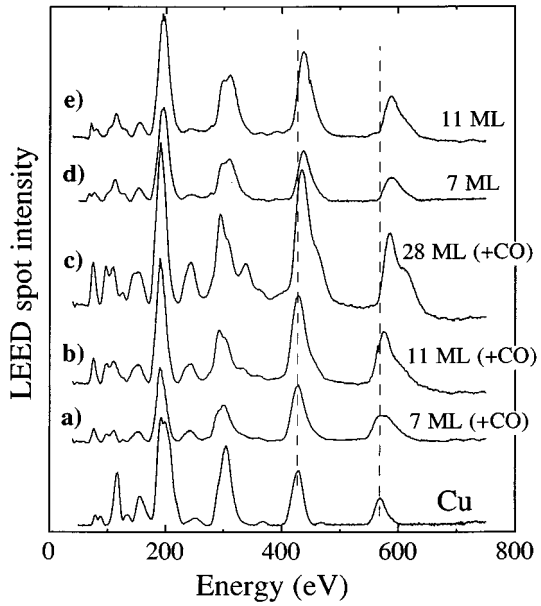

FIG. 10. I/V LEED curves [reflex (11)] for the Cu substrate and Fe films of various ML in thickness and differently prepared. For the CO-assisted growth the exposure of 0.3 L/ML was used. Relative shifts of the highest two energy peaks in (a)–(c) indicate the gradual relaxation of the interplanar spacing, which is consistent with the carbon incorporation model discussed in the text. Note that the final spacing is the same as that visible at any stage in the non-carbon-assisted case (d) and (e).

tions of the main peaks in I/V LEED curves indicate the interplanar distance of the sample. The shift of the main peaks of our data (Fig. 10) for clean films with respect to the Cu substrate demonstrates the structural relaxation to a smaller lattice constant.[14] In CO-stabilized films this shift is practically canceled in the same thickness region. Then stabilization is accompanied by lattice expansion (also applicable to hydrocarbons, see above), implying interstitial carbon incorporation as the interstitial carbon increases the lattice constant of the Fe-C solution.[3]

It should also be pointed out here that for CO-assisted growth the lattice expansion is much stronger than that for acetylene at the same carbon concentration. This fact becomes evident in comparing I/V LEED (Figs. 5 and 10) and Auger data (Figs. 3 and 8) of both cases. CO is probably more effective in the interstitial carbon incorporation. The reason for this effect might be in the floating oxygen layer: improving the interlayer transport and surface mobility, it probably promotes homogeneous carbon distribution and prevents it from forming precipitates. There is also a significant difference in the dissociation between CO and hydrocarbons: the incomplete dehydrogenation of ethylene and acetylene might prevent the interstitial incorporation.

As mentioned above, the STM images of these CO-stabilized film surfaces qualitatively show the same picture over the whole region 0–30 ML [see Fig. 7 (top)]. The growth is characterized by a smaller size of the islands than in the nonassisted case. This is in agreement with larger amplitudes of the MEED oscillations observed for this case (Fig. 6). In addition, as there is a layer of oxygen floating on the surface, the smaller island sizes indicate the role of oxygen as a surfactant[49] [compare also Ref. 38, where homoepitaxy on Pt(111) was studied]. Thus the difference between the effect of CO and that of hydrocarbons explains itself: both include the stabilizing effect of carbon, but only for CO does the growth proceed in a really good layer-by-layer mode, owing to the surfactant effect of oxygen.

Considering now thicker films, we find that the interplanar distance is reduced to the value of the nonassisted growth (compare the curve for 28 ML of the CO-stabilized film with those for 7 and 11 ML of the clean-grown films in Fig. 10). This change directly correlates with carbon disappearing from the top layers of the film. Obviously, at this thickness the film is already close to the approaching phase transformation, probably proceeding here because of the lack of carbon. In clean-grown films such incipient transformation can be noticed owing to bcc phase precipitates (needles).[10] Those needles are believed[10] to be responsible for the structural relaxation in clean-grown films. For carbon-assisted growth the origin of relaxation is not yet clear. Even at 30 ML it is

impossible to foresee the closely approaching phase transformation as the STM does not reveal any transformation precursor. Then suddenly the transformation takes place, and the surface roughness jumps by an order of magnitude (see insets in Fig. 7). The accumulating stress is probably the intrinsic reason for that sudden transformation: the strain energy increases with thickness until at some point the dislocation formation launches the whole transformation process.

C. Only oxygen

With the oxygen layer ''floating'' on top of the grown film and with no carbon in the larger part of it, oxygen might be assumed to mainly contribute to the stabilizing effect, while carbon is actually unimportant and might be omitted. To prove this hypothesis wrong a series of film growths under different partial pressures of oxygen has been performed.

However, the result of this investigation is only negative, as neither stabilization nor growth were improved at oxygen exposures up to 1 L/ML. Adsorbed oxygen is known to dissociate and form a regular $c(2\times2)$ pattern on many metal surfaces. The same applies to fcc iron, both on stable surfaces and during film growth. A layer of oxygen was shown to improve the initial growth mode of iron films.[4,39] In our study, no respective special investigations have been carried out. A slight increase of the first MEED peak might be due to this effect (this is the same kind of effect we observed for hydrocarbons).

The $c(2\times2)$ superstructure pattern appearing in the LEED images coincides with that obtained by either saturation of the clean film with O_2, or growth with CO also quantitatively, i.e., their I/V LEED data are identical.

Naturally, Auger spectra of these oxygen-assisted films reveal an oxygen peak, the strength of which depends on the by oxygen pressure applied. At the same time, the carbon peak is significantly suppressed, and at higher oxygen pressures (above 10^{-8} mbar) it is not measurable at all. Note that in the clean growth this carbon contamination is quite noticeable (1–2 at. %). Thus the oxygen blockade prevents any contamination of the grown film (except, of course, oxygen itself).

We now sum up our findings. (i) Carbon (partly) removes the intrinsic thermodynamic instability of the γ-Fe phase, thus creating the possibility of growing thicker films. However, it destroys the growth mode. (ii) On the other hand, oxygen does not stabilize the structure (see also the next section), but acting as a surfactant it compensates the destructive effect of carbon. Thus these two components help us to grow thick films of the γ-Fe phase of high-quality structure and surface morphology. (iii) However, the oxygen layer also plays a negative role: it blocks the surface of the growing film, thus preventing further carbon uptake. This fact suggests the existence of some balance between surfactant and ''poisoning'' effects of oxygen.

Hence it is obvious that observation (ii) simply is the common action of (i) and (iii), i.e., carbon and oxygen are working separately, being responsible for different aspects of the process. Thus, (i) + (iii) can be combined in another way, to enhance the growth by adding the mixture of gases. The following subsection is devoted to the results of such an experiment.

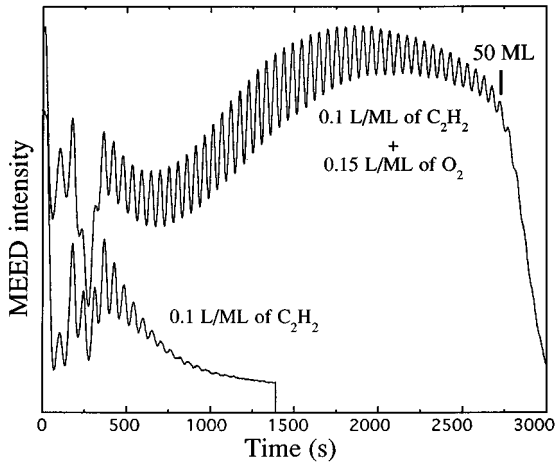

FIG. 11. MEED oscillation curve for the (acetylene + oxygen)-assisted grown film relative to that for the only-acetylene-assisted growth. The exposures used in the growth are indicated in the figure.

D. Deposition with $C_2H_2 + O_2$

Figure 11 shows the MEED data for (a) acetylene-assisted growth and (b) (acetylene + oxygen)-assisted growth, with the same partial pressure of acetylene being applied. The effect of oxygen is really impressive: a 50 ML thick film of excellent surface quality is easily produced. Again, the initial MEED intensity is almost recovered in the region of about 30 ML. Qualitatively, the growth properties (like contamination, surface structure, morphology, etc.) are exactly the same as for CO. At thicknesses above 40 ML the surface carbon contamination is small, whereas oxygen remains there forming the usual $c(2\times2)$ superstructure. Again the I/V LEED data (not shown here) indicate that the lattice expansion effect is stronger than that observed for the hydrocarbons alone (and having an even lower carbon concentration). Hence, similarly to CO, oxygen helps to incorporate the carbon interstitially. As mentioned above, hydrocarbons are not completely dissociated. Clearly, this excess of oxygen at the surface may considerably contribute to the complete carbon dehydrogenation and hence interstitial incorporation.

The sudden drop of the MEED intensity above 51 ML indicates the abrupt fcc→bcc transformation. The usual ''(3×1)'' LEED pattern occurs above that point.

However, there is one important difference here compared to CO: now the possibility arises of controlling the ratio between carbon and oxygen. Its significance is illustrated in Fig. 12. To the same partial pressure of acetylene different amounts of oxygen are added. Thus, if the oxygen exposure is too low, the surface quality degrades fast [Fig. 12(a)]. Increasing the exposure leads to a thicker film of better surface quality (b). However, excessive oxygen supply (c) blocks the carbon uptake too early, with the film quickly transforming to the bcc structure. Here, the balance between surfactant and ''poisoning'' effects of oxygen is clearly evident. As for CO this C-to-O ratio was strictly constant and the critical thickness proved to be pressure independent. Different acetylene and oxygen pressures could be tried, thus changing the C/O ratio from film to film and also during one

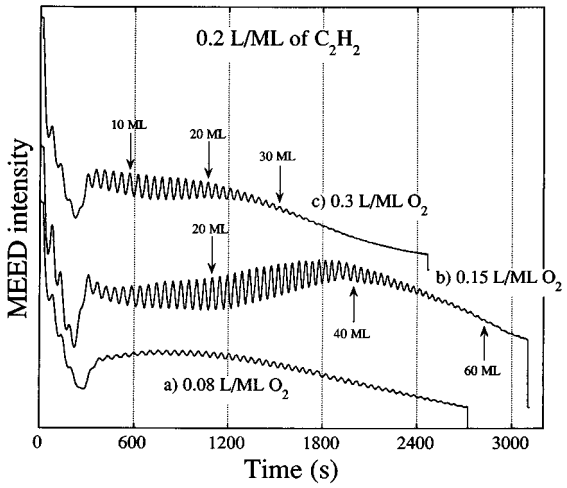

FIG. 12. MEED oscillation curves for (acetylene + oxygen)-assisted growth. The exposures are indicated in the figure. Blocking and surfactant effects of oxygen are demonstrated: (a) insufficient surfactant effect; (b) near optimum (for the given acetylene pressure); (c) the blocking effect is too strong.

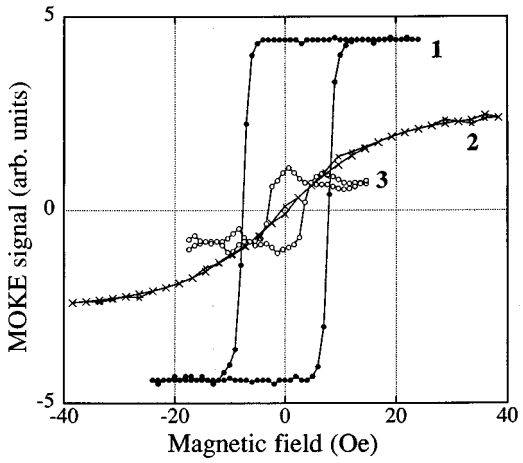

FIG. 13. MOKE hysteresis loops: (1) clean 3.5 ML film, polar geometry used indicating out-of-plane magnetization, $T = 260$ K; (2) 3.5 ML film including 14 at. % of carbon, polar geometry, and (3) the same sample measured in longitudinal geometry, the latter two taken at room temperature (300 K). This example shows that for a given thickness the magnetic easy axis may change from perpendicular to in plane with increasing carbon content. A corresponding phase diagram is given in Fig. 15 below.

growth process. Procedures of this kind, however, are beyond the scope of our consideration.

The MEED oscillations of Fig. 12(b) show that the iron film which is almost 70 ML thick still has the fcc structure (LEED studies also prove this). The following question naturally arises: where is the real stability limit of this system? Or in other words, what maximum critical thickness can be achieved with the help of the carbon incorporation? As discussed in the Introduction, the γ-Fe film instability is primarily due to the thermodynamic energy difference between fcc and bcc iron phases at RT. As soon as the interstitial carbon increases the γ-Fe stability region only a little,[28] the decrease of this energy loss can be supposed to be of the same order of magnitude, i.e., 20–30 % at the best. This decrease cannot explain the observed six- to sevenfold increase of the critical thickness. Therefore other factors have to be considered, too.

When the film is clean grown, at a thickness of about 4 ML there is a transformation between two different phases of γ-Fe (FM and AFM). This transformation is accompanied by a structural relaxation,[14] implying that in the region of 5–10 ML the films are no longer pseudomorphic. This transformation actually coincides with the appearance of bcc phase needles emerging as dislocations relaxing the structure.[10] These bcc-needles are in fact the origin of the incipient fcc $\rightarrow$bcc transformation. In contrast to that, however, in CO-[or (C+O)-] assisted growth such embryos do not occur, which might be due to the following reasons: (i) the films are still pseudomorphic owing to the carbon-induced lattice expansion, and (ii) the incorporated carbon inhibits the bcc phase formation even in the presence of dislocations. In spite of the bcc phase being still more favorable than the C-Fe fcc one, this ratio might be different in a narrow region along the dislocations. Therefore inhibiting the precipitate formation helps extend the γ-Fe stability range at least by a factor of 6. However, precise structural calculations are necessary to draw any definite conclusions.

III. MAGNETISM

Now the initial aim, viz., the magnetic properties of the films, will be recalled and discussed. Two questions arise: how does the carbon influence the magnetism of iron, and what are the magnetic properties of thick fcc Fe films? First, the magnetic properties of thin films (2–8 ML) grown with acetylene will be described, followed by those of thicker films (10–60 ML) stabilized with the help of CO or a $C_2H_2 + O_2$ mixture.

A. Carbon only (for film thicknesses of 2–8 ML)

For the magnetic characterization hysteresis curves are taken with the help of a standard MOKE setup. Figure 13 (curve 1) shows one example, measured on a 3.5 ML thick iron film at 260 K. From the set of such curves the thickness dependence of the saturation magnetization M_s was derived extrapolated to zero temperature (which is proportional to the magnetization of the film, at least in regions of low thickness), and so was the Curie temperature T_C of our samples. T_C was considered the temperature where the remanent magnetization becomes zero (see the discussion in Ref. 50).

Figure 14 shows the thickness dependencies of T_C and M_s measured on two different sets of samples: ''clean''-grown iron films and films obtained from acetylene-assisted growth. Auger spectra showed the presence of some 10–12 at. % carbon in the latter case. The curves are very similar. Slight differences (in both T_C and M_s) are probably due to the worse surface of the acetylene-assisted grown films. STM actually proves a quasi-three-dimensional surface, which, of course, influences the magnetism of surface layers. Hence the magnetic properties of the surface layer might probably also be changed by the carbon-induced surface reconstruction (see the LEED patterns in Fig. 4). However, as such changes are not observed for thicknesses below 4 ML, the question remains open. It is difficult to determine from only hysteresis measurements whether this drop in magnetization is due to the thinning of the magnetic surface layer (down to 1 magnetic ML) or to ''dead'' spots in the mag-

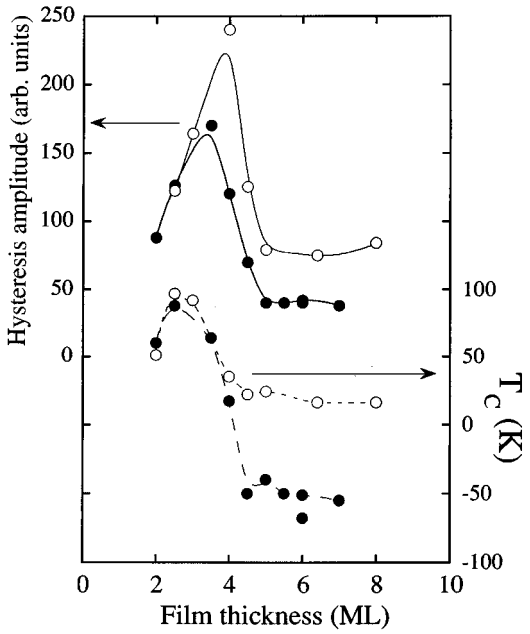

FIG. 14. Thickness dependence of the Curie temperature T_C (lower panel) and the Kerr ellipticities for saturation (which is proportional to M_s) extrapolated to T=0 K (upper panel) for fcc Fe films after ''clean'' preparation (open circles) and stabilized with C_2H_2 (solid circles), containing 10–12 at. % of carbon. In the latter case, a twice smaller value of M_s at thicknesses above 4 ML might be due to the thinning of the magnetic layer (down to 1 ML). The observed drop of T_C is in agreement with this effect.

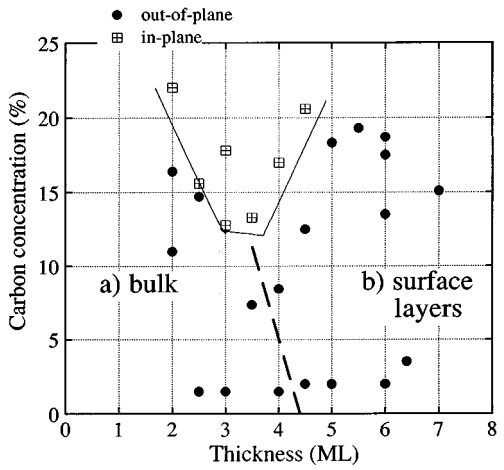

FIG. 15. Magnetic anisotropy phase diagram (film thickness versus carbon concentration) for γ-Fe films grown at a certain acetylene partial pressure. The solid line marks the region of in-plane anisotropy while the dashed one divides the out-of-plane anisotropy region into two parts: (a) the magnetization is homogeneous through the film and (b) only surface layers are magnetic.

netic bilayer. The change observed in the Curie temperature might be caused by either of these effects (or by both simultaneously).

These data allow the conclusion that incorporated carbon (at least up to a concentration of 10 at. %) does not considerably influence the bulk magnetic properties of the γ-Fe phase as long as all changes of magnetism seem to correlate with the surface changes.

However, increasing the carbon concentration implies a new effect. Figure 13 shows the behavior of out-of-plane (curve 2) and in plane (curve 3) hysteresis curves for an iron film of 3.5 ML in thickness containing 14 at. % of carbon. Now the magnetization clearly lies in the plane of the film. A kind of phase diagram is presented in Fig. 15, where the region of the in plane magnetization is shown as a function of film thickness and carbon concentration. In addition, the dashed line separates the out-of-plane magnetization region into two parts: at low thicknesses the films are homogeneously magnetized, while thicker films show the formation of magnetic surface layers.

Carbon seems to destroy the perpendicular anisotropy thus lowering the critical thickness where the magnetization switches to the surface. Therefore this critical thickness becomes lower than that of formation of the magnetic surface layers, whereas in ''clean''-grown films the latter form before the magnetization flips onto the surface.

Such a destruction might be a pure surface (or interface) effect, as it is the surface anisotropy term which turns the magnetization out of plane. Actually, the film structure seems to be unchanged as T_C is exactly the same as for perpendicularly magnetized samples of the same thickness; I/V LEED (see Fig. 5, curves for 3 ML thick films) does not show any structural change at this thickness.

The samples which in the phase diagram extend to the border between in-plane and out-of-plane regions show a reversible transition between in-plane magnetization at RT and out-of-plane magnetizaiton at lower temperatures. This effect can be compared with that demonstrated in Ref. 18. The difference is in the thickness range where this phenomenon is observed. However, in both cases the border concerned is between regions with in-plane and out-of-plane anisotropies. For low-temperature growth[18] no magnetic surface layers are observed to form, probably because of the completely different film morphology.[19] Therefore in thicker films the magnetization turns in-plane. Here, in contrast, the decrease of anisotropy lowers the critical thickness where this flip occurs.

Incidentially, magnetic studies indirectly evidenced the fact that even for thinner films carbon can be considered to be really *inside* the film. The sample contaminated from the top shows completely different magnetic behavior. If the carbon concentration is not very high (say, some 5–8 at. %), for 2–4 ML thick films grown with C_2H_2 a RT hysteresis loop is indistinguishable from the clean one. However, if the film was grown clean and then slightly contaminated from the top, we detect a noticeable increase (by several times) of coercive field. A magnetic aftereffect appears in such films[51] indicating the decrease of elementary magnetization reversal unity — the Barkhausen volume V_B. This decrease causes the rise of H_c. We find it surprising that this is not the case for acetylene-assisted grown films. This is, however, quite a subtle effect.

For a stronger surface contamination (1 L of acetylene on a 3 ML thick Fe film) the magnetism completely disappears (at least above 200 K). If the same exposure (or more) is used for the growth procedure, the film has its magnetic easy axis in plane, but the same Curie temperature.

Thus, carbon homogeneously distributed in the bulk has a different effect on the magnetic properties of iron than surface carbon does, which is quite difficult to understand. We suppose that surface carbon (or hydrocarbon species) ini-

tiates the formation of some clusters while this process is inhibited for incorporated atoms and molecules. At higher concentrations, these clusters might be able to destroy the magnetic percolation.

A brief conclusion may be drawn for the growth procedure. Namely, for correct magnetic studies of the Fe-C films the gas supply should be shut off strictly together with the end of film growth.

B. Carbon + oxygen

As the previous section showed, incorporated carbon only slightly influences the magnetic properties of the γ-Fe phase. Growing really thick films, however, requires some oxygen to be added, which will form an ordered layer on the surface. The influence of this oxygen on the magnetism is known to be negative. This effect can be easily checked on our iron films. Applying 1–2 L of O_2 to a clean film of 5–10 ML in thickness lowers the Curie temperature by at least 80–100 K. Nevertheless, this destructive effect is related to the surface only. If films thicker than 10 ML are investigated (we are interested, of course, in the bulk fcc Fe properties), the two topmost layers, which are destroyed by oxygen, can easily be neglected.

Thus hysteresis loops were measured for 10–60 ML thick iron films stabilized with CO or a $C_2H_2 + O_2$ mixture. All the samples appeared to be nonferromagnetic at temperatures above 180 K. At a certain point, increasing the film thickness for any growth regime leads to the fcc→bcc phase transformation and, at the same time, to the appearance of the bulk in plane film magnetization, with T_C being well above RT. This is a well-known property of the bcc phase. However, the absence of magnetization up to 60 ML (or even more) is observed and once more proves the fcc structure at these thicknesses.

CONCLUSION

In conclusion, we would like to briefly summarize our main results and emphasize the questions still open. The C-Fe phase diagram indicates the possibility of extending the stability region of the fcc phase of iron by adding a few at. % of carbon. This phase is supposed to be better stabilized in the form of a film epitaxially grown on Cu(001), if some carbon is added. Appropriate experiments have proved this assumption. Applying carbon is easy if different dissociative gases such as ethylene or acetylene are used. An important question remains open: where in the lattice is this carbon located? This can be answered only in part: part of this carbon is incorporated interstitially, as expected; whereas the other part probably forms some precipitates. To answer this question in more detail requires a precise film structure determination.

Next, an unusually strong surfactant effect has been discovered of oxygen in cooperation with carbon. The effect implies not only the improvement of the film morphology, but also the incorporation of carbon. The supposed mechanism is as follows. Regularly distributed oxygen increases the horizontal mobility of carbon. This helps to avoid the formation of precipitates and incorporate carbon more homogeneously.

An excess of oxygen largely reduces the stabilizing effect. The reason is very simple: a layer of oxygen blocks the surface so that no carbon can penetrate into the film. Thus the surfaces of very thick films are free of carbon. This carbon depletion appears to cause the structural transformation of the grown film. It is still not clear how this happens. In the film of 50 ML in thickness, the upper 15–20 ML contain carbon at the level of nonassisted growth. The point of interest is the morphology of such a film (measured by STM on the nanometer scale) which is different from the usual case. Again, the knowledge of the atomic-scale structure of the film is necessary to elucidate the difference.

A minor effect still very interesting occurring in our study is growth-induced CO dissociation, which is necessary for CO-induced stabilization.

However, the stabilizing mechanism itself is not yet entirely understood. We assume that the incorporated carbon prevents the formation of bcc phase precipitates, thus delaying the phase transformation, for which there are two reasons: (i) carbon expands the lattice, hence removing the dislocations which normally serve as nuclei for the bcc precipitates; (ii) interstitial carbon makes the formation of bcc precipitates less favorable (or not favorable at all).

As to the magnetic properties of those stabilized films, our results clearly are not exhaustive. They will be a topic for future experiments. The influence of incorporated carbon on the magnetic properties of fcc Fe was proven to be vanishing. On the other hand, the absence of FM order in thick ($\leqslant$ 70 ML) stabilized films is one more, though indirect, proof of their fcc structure.

As pointed out in the Introduction, there are now some indications that γ-Fe films are antiferromagnetic at $T<$ 200 K.[16] Strictly speaking, they are a kind of AFM wave with a 2.6 ML period. The short thickness range accessible (5–10 ML) was certainly not sufficient to definitely determinate the properties of that wave. Now we hope to offer possibilities for future experiments.

APPENDIX: DISCUSSION OF THE C-O SURFACE COVERAGE

As pointed out above, the growth with CO produces a film surface which is almost free of carbon, if the applied CO pressure is high enough. A simple model will help us to understand the behavior of the surface carbon and oxygen concentrations with respect to the film thickness. Let n be the number of molecules striking 1 cm^2 of the sample surface per second, and suppose the sticking coefficient to be unity for the molecules striking the clean Fe surface, and otherwise zero. N denotes the surface concentration of the oxygen atoms (including those in CO molecules). With no dissociation, N is simply the number of CO molecules on the surface. New molecules impinging on the surface will be absorbed at free surface sites, only:

$$dN = n\frac{N_0 - N}{N_0}dt, \tag{A1}$$

where N_0 is the total number of absorbing sites. Now, if the film is growing at rate R, dissociation will take place. It is probably proportional to R. N_C denotes the surface concentration of carbon atoms; in fact, this number coincides with the number of non-dissociated CO molecules. Thus the car-

bon concentration increases at the expense of the CO molecules sticking to the surface and decreases owing to dissociation:

$$dN_C = n\frac{N_0 - N}{N_0}dt - \alpha R N_C dt, \tag{A2}$$

with α being the factor of proportionality between growth rate and dissociation. At the same time, the number of surface oxygen atoms is not influenced by dissociation.

This simple system of equations (A1) and (A2) may be solved using the initial conditions $N(0)=0$, $N_C(0)=0$, yielding

$$N(t) = N_0(1 - e^{-(n/N_0)t}), \tag{A3}$$

$$N_C(t) = \frac{N_0}{1 - \alpha R\dfrac{N_0}{n}}(e^{-\alpha R t} - e^{-(n/N_0)t}). \tag{A4}$$

Thus these solutions contain only two parameters: the normalized CO partial pressure n/N_0, and the dissociation rate αR. The ratio between these two parameters determines the shape of the $N_C(t)$ behavior, while qualitatively $N(t)$ always remains the same. Figure 16 shows these curves for different values of the CO pressure applied (i.e., for different values of the n/N_0 ratio and the same dissociation rate parameter αR). A qualitative agreement with experimental data (compare Fig. 8) is obvious. As pointed out before, here only adsorption is assumed (probability 1 if the molecule strikes the clean Fe surface, and 0 otherwise) as well as dissociation proportional to the growth rate (i.e., time constant). To be more quantitative, one should also take into account desorption, the difference between the flat surface and steps, etc. The finite probing depth of the Auger technique will also influence the result. Nevertheless, even such a simple consideration could explain the general physical behavior.

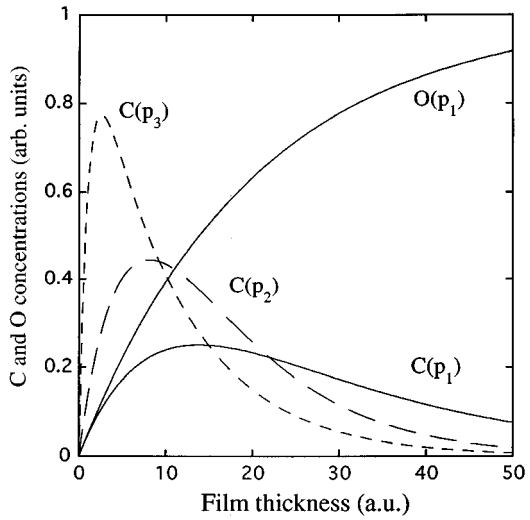

FIG. 16. Calculated [from formulas (A3)and (A4)] surface concentrations of carbon and oxygen versus film thickness for CO-assisted growth. Plotted are carbon and oxygen contents at the film surface obtained with different exposures of CO: $p_1<p_2<p_3$. Qualitative agreement with experimental data (Fig. 8) is obvious.

*Present address: EVSF 2, University of Nijmegen, Toernooiveld 1, 6525 ED Nijmegen, The Netherlands.

[1] V.L. Moruzzi, P.M. Marcus, K. Schwarz, and P. Mohn, Phys. Rev. B **34**, 1784 (1986).
[2] H.-J. Ernst and R. Folkers (unpublished).
[3] W.B.Pearson, *A Handbook of Lattice Spacing and Structures of Metals and Alloys* (Pergamon, New York, 1958).
[4] K.E. Johnson, D.D. Chambliss, R.J. Wilson, and S. Chiang, J. Vac. Sci. Technol. A **11**, 1654 (1993).
[5] J. Shen, J. Giergiel, A. Schmidt, and J. Kirschner, Surf. Sci. **328**, 32 (1995).
[6] M.T. Kief and W.F. Egelhoff, Jr., Phys. Rev. B **47**, 10 785 (1993).
[7] W.A. Jesser amd J.W. Matthews, Philos. Mag. **15**, 1097 (1967).
[8] H.A. Wierenga, W. de Jong, M.W.J. Prins, Th. Rasing, R. Vollmer, A. Kirilyuk, H. Schwabe, and J. Kirschner, Phys. Rev. Lett. **74**, 1462 (1995).
[9] K.S. Cheung and R.J. Harrison, J. Appl. Phys. **71**, 4009 (1992).
[10] J. Giergiel, J. Kirschner, J. Landgraf, J. Shen, and J. Woltersdorf, Surf. Sci. **310**, 1 (1994).
[11] J. Thomassen, F. May, B. Feldmann, M. Wuttig, and H. Ibach, Phys. Rev. Lett. **69**, 3831 (1992).
[12] H. Magnan, D. Chandesris, B. Villette, O. Heckmann, and J. Lecante, Phys. Rev. Lett. **67**, 859 (1991).
[13] S. Müller, P. Bayer, C. Reischl, K. Heinz, B. Feldmann, H. Zillgen, and M. Wuttig, Phys. Rev. Lett. **74**, 765 (1995).
[14] P. Bayer, S. Müller, P. Schmailzl, and K. Heinz, Phys. Rev B **48**, 17 611 (1993).
[15] J. Shen, J. Giergiel, and J. Kirschner (private communication).
[16] Dongqi Li, M. Freitag, J. Pearson, Z.Q. Qiu, and S.D. Bader, Phys. Rev. Lett. **72**, 3112 (1994).
[17] R. Allenspach and A. Bischof, Phys. Rev. Lett. **69**, 3385 (1992).
[18] D.P. Pappas, K.-P. Kämper, and H. Hopster, Phys. Rev. Lett. **64**, 3179 (1990); D.P. Pappas *et al.*, J. Appl. Phys. **69**, 5209 (1991).
[19] J. Giergiel, J. Shen, J. Woltersdorf, A. Kirilyuk, and J. Kirschner, Phys. Rev. B **52**, 8528 (1995).
[20] P. Xhonneux and E. Courtens, Phys. Rev. B **46**, 556 (1992).
[21] J.R. Dutcher, B. Heinrich, J.F. Cochran, D.A. Steigerwald, and W.F. Egelhoff, Jr., J. Appl. Phys. **63**, 3464 (1988).
[22] J.R. Dutcher, J.F. Cochran, D.A. Steigerwald, and W.F. Egelhoff, Jr., Phys. Rev. B **39**, 10 430 (1989).
[23] D. Pescia, M. Stampanoni, G.L. Bona, A. Vaterlaus, R.F. Willis, and F. Meier, Phys. Rev. Lett. **58**, 2126 (1987).
[24] T. Ezawa, W.A.A. Macedo, U. Glos, W. Keune, K.P. Schletz, and U. Kirschbaum, Physica B **161**, 281 (1989).
[25] A. Onodera, Y. Tsunoda, N. Kunitomi, O.A. Pringle, R.M. Niklow, and R.M. Moon, Phys. Rev. B **50**, 3532 (1994).
[26] B. Feldmann, A. Sokoll, and M. Wuttig (unpublished).
[27] M. T. Lin, J. Shen, J. Giergiel, W. Kuch, H. Jenniches, M. Klaua, C.-M. Schneider, and J. Kirschner (unpublished).
[28] O. Kubaschewski, *Iron—Binary Phase Diagrams* (Springer-Verlag, Berlin, 1982).
[29] H. Akai, M. Takeda, and J. Kanamori, *Research Report on Metallic Artificial Superlattice* (Tokyo University, Tokyo, 1994), p. 215.
[30] G.Y. Chin and J.H. Wernik, in *Ferromagnetic Materials*, edited

by E.P. Wohlfarth (North-Holland, Amsterdam, 1986), Vol. 2, p. 55.
[31] M. Erley, A.M. Baro, and H. Ibach, Surf. Sci. **120**, 273 (1982).
[32] T.N. Rhodin, C.F.Brucker, and A.B. Anderson, J. Phys. Chem. **82**, 894 (1978).
[33] A.J. Slavin, B.E. Bent, C.-T. Kao, and G.A. Somorjai, Surf. Sci. **206**, 124 (1988).
[34] L. Hanley, Z. Xu, and J.T. Yates, Jr., Surf. Sci. **248**, L265 (1991).
[35] A limited, 2–3 ML CO-induced extension of fcc growth range has been reported by Thomassen *et al.* (Ref. 11).
[36] Dongqi Li, M. Freitag, J. Pearson, Z.Q. Qiu, and S.D. Bader, J. Appl. Phys. **76**, 6425 (1994).
[37] H. den Daas, E.H. Voogt, O.L.J. Gijzeman, and J.W. Geus, Surf. Sci. **306**, 1 (1994).
[38] S. Esch, M. Hohage, T. Michely, and G. Comsa, Phys. Rev. Lett. **72**, 518 (1994)
[39] D.A. Steigerwald, I. Jacob, and W.F. Egelhoff, Jr., Surf. Sci. **202**, 472 (1988).
[40] A. Kirilyuk, J. Giergiel, J. Shen, and J. Kirschner, Phys. Rev. B **52**, R11 672 (1995).
[41] J. Giergiel, H. Hopster, J.M. Lawrence, J.C. Hemminger, and J. Kirschner, Rev. Sci. Instrum. **66**, 3474 (1995).
[42] H. Glatzel, Th. Fauster, B.M.U. Scherzer, and V. Dose, Surf. Sci. **254**, 58 (1991).
[43] A.B. Hayden, P. Pervan, and D.P. Woodruff, Surf. Sci. **306**, 99 (1994).
[44] K. Kalki, D.D. Chambliss, K.E. Johnson, R.J. Wilson, and S. Chiang, Phys. Rev. B **48**, 18 344 (1993).
[45] T.J. Vink, O.L.J. Gijzeman, and J.W. Geus, Surf. Sci. **150**, 14 (1985).
[46] O.P. van Pruissen and O.L.J. Gijzeman, Appl. Surf. Sci. **27**, 52 (1986).
[47] O.L.J. Gijzeman, T.J. Vink, O.P. van Pruissen, and J.W. Geus, J. Vac. Sci. Technol. A **5**, 718 (1987).
[48] I. Ganzmann, W. Kiessling, D. Borgmann, and G. Wedler, Surf. Sci. **269/270**, 347 (1991).
[49] J. Tersoff, A.W. Denier van der Gon, and R.M. Tromp, Phys. Rev. Lett. **72**, 266 (1994).
[50] R. Allenspach, J. Magn. Magn. Mater. **129**, 160 (1994).
[51] A. Kirilyuk, J. Giergiel, J. Shen, and J. Kirschner, J. Magn. Magn. Mater. (to be published).